(12)

DAVID W. TAYLOR NAVAL SHIP RESEARCH AND DEVELOPMENT CENTER

Bethesda, Md. 20084

SPD-718-02

AD A046416

FULL SCALE EVALUATION OF WATERJET PUMP IMPELLERS

AD No. ____
DDC FILE COPY

FULL SCALE EVALUATION OF WATERJET PUMP IMPELLERS

by

Reuel S. Alder

and

Stephen B. Denny

APPROVED FOR PUBLIC RELEASE: DISTRIBUTION UNLIMITED

SHIP PERFORMANCE DEPARTMENT

September 1977

SPD-718-02

MAJOR DTNSRDC ORGANIZATIONAL COMPONENTS

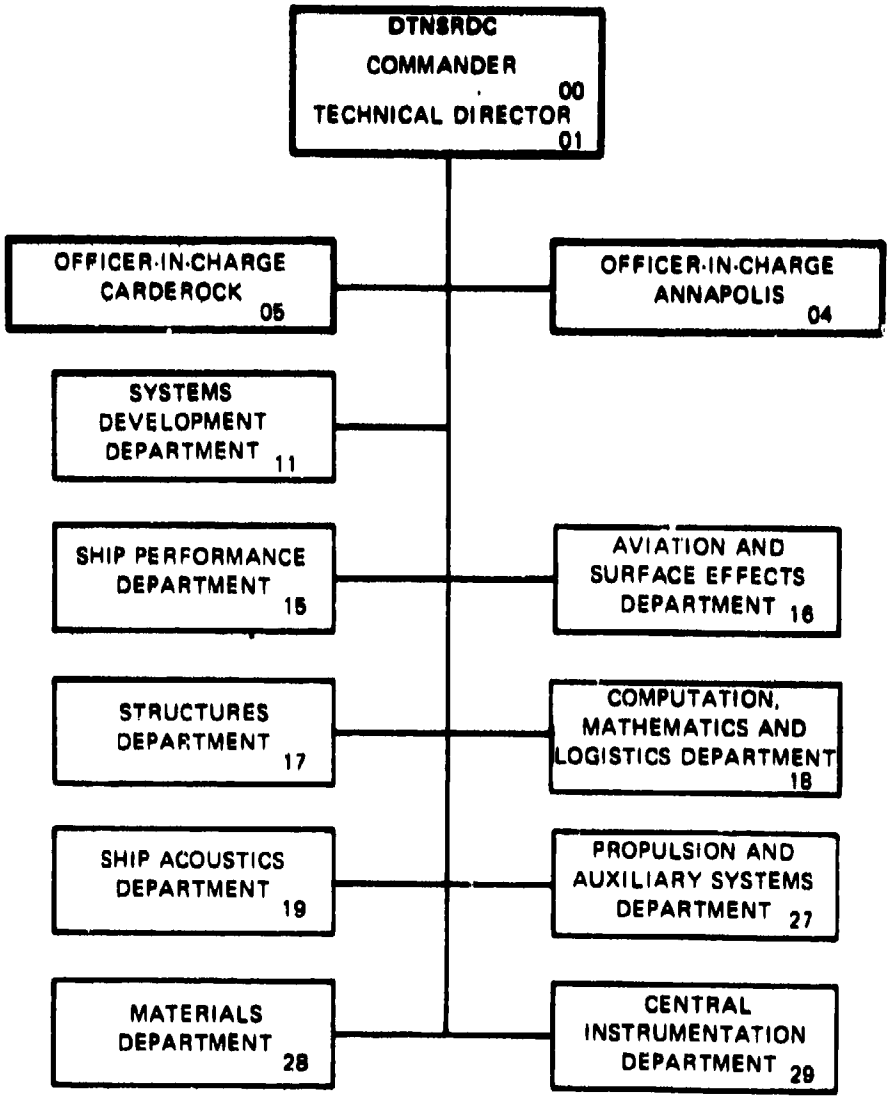

UNCLASSIFIED

SECURITY CLASSIFICATION OF THIS PAGE *(When Data Entered)*

REPORT DOCUMENTATION PAGE

READ INSTRUCTIONS BEFORE COMPLETING FORM

1. REPORT NUMBER: SPD-718-02	2. GOVT ACCESSION NO.
3. RECIPIENT'S CATALOG NUMBER	
4. TITLE (and Subtitle): Full Scale Evaluation of Waterjet Pump Impellers	5. TYPE OF REPORT & PERIOD COVERED
	6. PERFORMING ORG. REPORT NUMBER
7. AUTHOR(s): Reuel S. Alder and Stephen B. Denny	8. CONTRACT OR GRANT NUMBER(s)
9. PERFORMING ORGANIZATION NAME AND ADDRESS: David W. Taylor Naval Ship R&D Center, Bethesda, Maryland 20084	10. PROGRAM ELEMENT, PROJECT, TASK AREA & WORK UNIT NUMBERS: Program Element 62756N, Task Area ZF 61 412 001, Work Unit 1532-021
11. CONTROLLING OFFICE NAME AND ADDRESS	12. REPORT DATE: September 1977
	13. NUMBER OF PAGES: 49
14. MONITORING AGENCY NAME & ADDRESS *(if different from Controlling Office)*: F61412	15. SECURITY CLASS. *(of this report)*: UNCLASSIFIED
	15a. DECLASSIFICATION/DOWNGRADING SCHEDULE

16. DISTRIBUTION STATEMENT *(of this Report)*: ZF61412001

APPROVED FOR PUBLIC RELEASE; DISTRIBUTION UNLIMITED

DDC REGISTERED NOV 16 1977 B

17. DISTRIBUTION STATEMENT *(of the abstract entered in Block 20, if different from Report)*

18. SUPPLEMENTARY NOTES

19. KEY WORDS *(Continue on reverse side if necessary and identify by block number)*
Waterjets
Flush Inlet Waterjets
Internal Flow Measurement
Full Scale Evaluation

20. ABSTRACT *(Continue on reverse side if necessary and identify by block number)*

Full scale experiments were conducted with a U. S. Navy waterjet-powered planing boat to evaluate three different waterjet impeller/nozzle configurations. The configurations consisted of the standard impeller/nozzle combination currently installed on these craft in addition to a newly designed impeller evaluated with two different diameter nozzles.

DD FORM 1 JAN 73 1473 EDITION OF 1 NOV 65 IS OBSOLETE
S/N 0102-014-6601

UNCLASSIFIED
SECURITY CLASSIFICATION OF THIS PAGE *(When Data Entered)*

389 694

20.

The overall program objective was to determine if marine propeller design techniques can be applied to the design of waterjet impellers and thereby improve (impeller) efficiency. The purpose of the experimentation was to obtain data necessary for an impeller design, e.g., impeller power absorption and inlet velocity inflow characteristics. A first-cut impeller design was constructed and evaluated in the experiments in addition to the standard impeller.

Results of the experimental program have been reported in this report and in Reference 2. These results show that the waterjet with a newly designed impeller approached but did not meet or exceed the overall performance of the waterjet equipped with the standard impeller and nozzle. The inlet velocity measurements showed extreme local velocity variations in flow approaching the impeller suggesting that any improvement in the impeller would have a marginal improvement on overall performance of the waterjet.

It is concluded that marine propeller design techniques cannot be practically applied to the design of waterjet impellers in the majority of waterjets where extremely high thrust (disk loading) conflicts with the moderately-loaded propeller theory upon which the design procedures are based.

TABLE OF CONTENTS

LIST OF FIGURES

LIST OF TABLES

NOTATION

A_D	Developed blade area	ft^2, m^2
A_E	Expanded blade area	ft^2, m^2
A_j	Area of exit nozzle	in^2, m^2
A_o	Impeller disc area $\pi D^2/4$	ft^2, m^2
c	Chord length	ft, m
D	Impeller maximum diameter	ft, m
f_M	Blade section camber	ft, m
g	Acceleration due to gravity	ft/sec^2, m/s^2
J_A	Propeller advance coefficient, $J_A = V_A/nD$	
n	Shaft revolution rate	rev/sec
P	Impeller blade section pitch	ft, m
p_{atm}	Atmospheric pressure	psia, Pa
p_d	Dynamic pressure, $p_d = p_t - p_s$	psia, Pa
p_s	Local static pressure	psia, Pa
p_t	Local total pressure, $p_t = p_s + 1/2\rho V_i^2$	psia, Pa
Q	Pump volume flow rate	ft^3/sec, m^3/sec
r	Local radius	ft, m
R	Nozzle radius or impeller maximum radius	ft, m
t	Maximum blade section thickness	ft, m
T_b	Bollard measured thrust	lb, N
T_n	Net thrust underway, $T_n = \rho Q^2/A_j - \rho Q V_s$	lb, N

V_A	Propeller advance velocity	ft/sec, m/s
V_C	Velocity of carriage	ft/sec, m/s
V_i	Local upstream velocity	ft/sec, m/s
V_j	Average nozzle velocity	ft/sec, m/s
V_p	Velocity computed from pressure probe measurements	ft/sec, m/s
V_s	Boat velocity	knots
$1 - w_o$	Nominal wake factor , $1 - w_o = V_A/V_s$	
$1 - w_x$	Local wake factor , $1 - w_x = V_i/V_s$	
x	r/R	
Z	Number of blades of a propeller	
α	Inflow angle to probe	degrees
ρ	Density of fluid	$lbf\text{-}sec^2/ft^4$, Kg/m^3

ABSTRACT

Full scale experiments were conducted with a U.S. Navy waterjet-powered planing boat to evaluate three different waterjet impeller/nozzle configurations. The configurations consisted of the standard impeller/nozzle combination currently installed on these craft in addition to a newly designed impeller evaluated with two different diameter nozzles.

The overall program objective was to determine if marine propeller design techniques can be applied to the design of waterjet impellers and thereby improve (impeller) efficiency. The purpose of the experimentation was to obtain data necessary for an impeller design, e.g., impeller power absorption and inlet velocity inflow characteristics. A first-cut impeller design was constructed and evaluated in the experiments in addition to the standard impeller.

Results of the experimental program have been reported in this report and in Reference 2. These results show that the waterjet with a newly designed impeller approached but did not meet or exceed the overall performance of the waterjet equipped with the standard impeller and nozzle. The inlet velocity measurements showed extreme local velocity variations in flow approaching the impeller suggesting that any improvement in the impeller would have a marginal improvement on overall performance of the waterjet.

It is concluded that marine propeller design techniques cannot be practically applied to the design of waterjet impellers in the majority of waterjets where extremely high thrust (disk loading) conflicts with the moderately-loaded propeller theory upon which the design procedures are based.

ADMINISTRATIVE INFORMATION

This work was carried out under Independent Exploratory Development (IED) program funding. Project identification was Program Element 62756N, Task Area ZF 61 412 001, Work Unit 1532-021.

INTRODUCTION

Waterjet propulsion systems have application where appendage and draft restrictions are critical to maneuverability and overall craft performance. A limitation of waterjet application is their lower efficiency when compared to marine screw propellers[1]. Reduced efficiency in waterjet systems may come from inlet, duct, impeller, stator, and nozzle losses and from losses due to raising the water from an inlet level to the level of the exit nozzle.

This in-house (Independent Exploratory Development) program was initiated to determine the potential for increasing waterjet efficiency by improvement of impeller design technology. Specifically, the task was to determine whether or not marine propeller design procedures could be used to design and consequently improve the efficiency of a waterjet impeller. The tools to be considered were lifting line and lifting surface propeller design procedures which have reached a high degree of sophistication in recent years. For

---

[1] Brandau, J. H., "Performance of Waterjet Propulsion Systems - A Review of the State-of-the-Art," Journal of Hydronautics, Vol. 2, No. 2, pp. 61-76 (April 1968).

marine propellers, these procedures allow design for given thrust production or horsepower absorption at desired shaft revolution rate and with a minimum of cavitation. Since marine propellers are axial flow devices, an obvious candidate for impeller design improvement would be an axial flow (preferably single stage) waterjet.

In the initial stages of the program it was apparent that two major requirements were (1) a vehicle and/or a set of operating conditions for which to conduct the propulsor design and (2) a mechanism on which the product (presumably a waterjet impeller) could be experimentally evaluated. The only craft which met both of these requirements and which was available within the desired time frame was a 31-ft (9.45 m) 15,600 lb (69,392 N) planing craft maintained by the Naval Ship Engineering Center, Norfolk Division (NAVSECNORDIV). The craft is equipped with two flush inlet waterjets. The waterjet is a single stage (one impeller and one set of stator vanes) waterjet unit with near axial flow through the impeller plane. Craft availability along with acceptable waterjet internal geometry led to its selection to fulfill requirements (1) and (2) above.

A requirement in utilizing current marine propeller design procedures is knowledge of the inflow characteristics into the propeller (impeller) plane and the power absorbed or thrust produced by the propeller. Since no adequate information of this type was available, the experimental program described in this report and

in Reference 2 was undertaken.

A "first-cut" impeller design was generated and the unit was constructed for evaluation along with the standard waterjet impeller. A description of this impeller design is included in this report along with the results of the experimental evaluation of both waterjet impellers.

DESCRIPTION OF APPARATUS

Experiments were conducted using a 31-ft (9.45 m) planing craft described in Table 1 and propelled by two waterjets. The waterjets are single stage mixed flow pumps powered by separate diesel engines rated at 216 hp (161 kW) each at 2800 rpm. Two impellers, one of standard design and one of new design, were provided for the starboard waterjet along with two nozzles of different diameter that were interchanged during the experiments. Instrumentation installed and maintained by NAVSECNORDIV was included on the starboard waterjet to measure torque, rpm, and internal pressures in the bell housing aft of the impeller. The port waterjet operated in its normal configuration. A description of the standard waterjet dimensions and ducting profile is found in Figure 1. The cutting plane AA shown in Figure 1 was the location of two traversing pressure probes designed to measure static and total head pressures. Cross section AA is

---

[2] Alder, R. S., "Inlet Velocity Distribution of a Full Scale Flush Inlet Waterjet," DTNSRDC Ship Performance Department Report SPD-718-01 (Aug 1976).

described in more detail in Figure 2 and the 11 vertical positions at which the upstream pressure measurements were made are designated. The waterjet inlet and grating has been defined in Figure 3.

Two separate impellers as described in Tables 2 and 3 were evaluated in the starboard waterjet. Table 2 describes the standard waterjet impeller and Table 3 is a description of the DTNSRDC impeller designed for the waterjet using propeller design considerations. Two separate nozzles were used during the experiments, the standard 5.75 in. (0.146 m) diameter nozzle and a 6.0 in. (0.1524 m) diameter nozzle.

The two upstream probes were traversed vertically across the duct while another probe traversed the exit nozzle horizontally. A detailed description of these probes is given in Reference 2.

IMPELLER SELECTION

The primary objective of the overall research program was to determine whether or not marine propeller design techniques could be applied to the design of waterjet impellers and thereby improve their (impeller) efficiency. The design tools available included lifting line[3]

---

[3] Lerbs, H. W., "Moderately Loading Propellers with a Finite Number of Blades and an Arbitrary Distribution of Circulation," Trans. SNAME, Vol. 60, pp. 73-117 (1952).

and lifting surface propeller design procedures[4,5,6] and a ducted propeller design method[7].

Before a detailed single point impeller design could be carried out, some preliminary experimentation was necessary to provide input for the design. In particular, inflow characteristics and impeller power absorption as functions of craft speed and shaft rpm were quantities necessary for the initial design stages. Since full scale experimentation to obtain this information is involved and costly, it was decided that a "first-cut" impeller design would be derived, constructed, and evaluated along with the standard impeller during these full scale experiments. Although it was known that the "first-cut" design could not be highly sophisticated, it appeared that potential improvement of the standard impeller geometry could be made in the areas of cavitation performance and increased mass flow rates at sustained power levels. Following is a step by step description

---

[4] Cheng, H. M., "Hydrodynamic Aspect of Propeller Design Based on Lifting-surface Theory, Part I, Uniform Chordwise Load Distribution," David Taylor Model Basin Report 1802 (Sep 1964).

[5] Cheng, H. M., "Hydrodynamic Aspect of Propeller Design Based on Lifting-Surface Theory, Part II, Arbitrary Chordwise Load Distribution," David Taylor Model Basin Report 1803 (Jun 1965).

[6] Kerwin, J. E. and R. Leopold, "Propeller-Incidence Correction Due to Blade Thickness," J. Ship REsearch, Vol. 7, No. 2 (Oct 1963).

[7] Caster, E. B., "A Computer Program for Use in Designing Ducted Propellers," Naval Ship Research and Development Center Report 2507 (Oct 1967).

of the new impeller design. Justifications for each step and assumptions made during the process are included.

It was assumed that the new impeller geometry might differ from that of the standard impeller in blade area, blade number, and the radial distribution of blade section pitch, camber, and chord length. However, since the standard waterjet unit configuration had been widely utilized and had acceptable performance when compared to waterjets in general, it was also assumed that the "first-cut" impeller design geometry would not vary radically from that of the standard impeller. For these reasons the standard impeller geometry was carefully measured to establish a baseline "parent" for the new design. Representative geometric characteristics determined through that measurement are presented in Table 2.

The next stage of the impeller design process was an extensive investigation with the ducted propeller design program[7]. This program consists of a propeller lifting line design theory coupled with a calculation procedure for determining the induced flow (mutual interaction) between an annular duct and a contained propeller. As it exists, the program requires as input those quantities normally required for a lifting line theoretical design (i.e., absorbed power or desired thrust, inflow characteristics, propeller rotation rate, blade chord lengths, blade number, and propeller diameter) in addition to the description of the annular duct. Duct geometries handled by

the program are body-of-revolution types with the axis of revolution corresponding to the propeller axis. Duct length, thickness, and section profile shape are input parameters along with the propeller tip clearance and a duct frictional drag coefficient if desired. Since a craft-installed flush inlet waterjet bears little resemblance to an annular duct, a simple representative duct shape was chosen for the ducted propeller program calculations. The simplified duct considered had a length of six impeller diameters, no contractions, zero frictional drag, and zero thickness. The input to the propeller portion of the program consisted of the blade area distribution and blade number of the standard "parent" impeller. In addition, the power/rpm limits of one of the test craft power plants was input, e.g, 216 horsepower (161 kW) at 2800 rpm. To satisfy a program input requirement for inflow characteristics, a craft speed (V_s) and local wake distribution were entered such that the total integrated mass flow (neglecting duct and impeller induced velocities) was 85% of the mass flow value deemed necessary to drive the craft at peak speed.

The resulting computations produced an impeller design with extremely high blade pitch and camber when compared to the standard parent impeller. In view of these results, the following conclusions were made:

1. The high horsepower (216) prescribed for impeller absorption exceeded the capabilities of the moderately-loaded propeller theory upon which the design procedure was based and/or

2. The flow velocity within the waterjet inlet is induced almost entirely by the impeller and duct.

In retrospect both conclusions (1) and (2) seemed highly logical. The calculated duct-induced axial velocities produced at the impeller plane were approximately 10% of the craft speed and varied from near 0.07 V_s at the impeller blade roots to 0.13 V_s at the blade tips. It was apparent that the impeller induced velocities would account for a much higher percentage of the inflow velocity.

At this stage of the new impeller design development, an alternate approach was taken. The duct induced wake distribution previously calculated was assumed to be valid corresponding to an impeller power absorption of 216 hp (161 kW). The ducted propeller design program was abandoned in favor of the easier-to-use conventional propeller lifting-line design procedure. Calculations were performed using the same input as in the ducted propeller computations except for the local wake distribution which was chosen to be that distribution (and magnitude) produced by the duct (from previous calculations). Results from these calculations showed that geometric pitch and camber were less than those computed with the ducted propeller program (in which propeller advance velocity was based on estimated waterjet mass flow) but blade pitch and camber values were still significantly higher than those of the standard parent propeller. These results led to the assumption that both previous conclusions (1) and (2) were probably valid and a consequent third approach was then taken.

Using the duct induced flow distribution as the only inflow velocities not produced by the impeller, a series of propeller designs was generated in which all input remained the same except for absorbed power which was successively reduced by incremental values from peak value of 216 hp (161 kW) to a low of 108 hp (80.5 kW). For each of the impeller (propeller) designs thus generated, lifting-surface corrections were applied to the lifting-line calculated design results to determine the final geometry of propellers which could be expected to absorb the prescribed power levels at the designated operating advance condition. From interpolation within the propeller series, it was determined that the standard "parent" impeller geometry represented a propeller which would absorb, in the absence of cavitation, approximately 131.3 hp (97.9 kW) at 2800 rpm and at an advance coefficient, $J_A = 0.1$. With this information it was now possible to proceed with a new impeller design which would vary somewhat in geometry from the standard impeller and, hopefully, display better cavitation performance and an increased mass flow rate at the same absorbed power.

In order to delay the onset of cavitation and possibly reduce the extent of cavitation for the new impeller at its design operating point, it was decided to design the impeller for a Lerbs optimum radial distribution of pitch matched to the anticipated wake distribution. In conventional propeller designs for heavily-loaded operating conditions,

blade sections near the propeller tip may be pitched below that prescribed by Lerbs optimum distribution in order to reduce local blade tip loading and delay the onset of tip vortex and blade cavitation. Since the waterjet impeller blade tips operate in close proximity to a solid boundary, however, the impeller blade outer sections should maintain a larger percentage of blade loading than is the case for conventional propellers. Therefore, no reduction in blade pitch near the tips was deemed necessary. The radial distribution of axial inflow selected for the design was that calculated with the ducted propeller program for the condition of 216 absorbed hp (161 kW). This distribution $(1 - w_x)$ varied from 0.07 at the impeller blade root to 0.13 at the blade tip and the integrated nominal wake fraction $(1 - w_o)$ was approximately = 0.1. The radial distribution of blade pitch computed in this manner and for the prescribed wake distribution produced blade pitch-to-diameter ratios, P/D, greater in magnitude at the tip than at the hub. From Table 2 it is apparent that this trend is opposite to the P/D radial distribution of the standard impeller.

The second area for potential improvement in impeller performance (over that of the standard impeller) was that of increasing mass flow through the impeller disk while maintaining absorbed power levels. An inspection of propeller series open-water test data showed that at low advance ratios, $J_A = V_A/nD \approx 0.1$, four-bladed propellers are more

efficient thrust producers than three-bladed propellers of the same total blade area ratio, A_E/A_o. By equating propeller thrust production to waterjet impeller mass flow production, it appeared that a four-bladed impeller might produce 3 - 4% higher mass flow rates than a three-bladed impeller with all other things being equal. With these potential improvements in mind, a new four-bladed impeller was designed based on the following criteria:

Diameter = 0.988 ft (0.301 m)

RPM = 2800

Shaft Power = 131.3 hp, 97.9 kW

V_s = 50.63 ft/sec, 15.43 m/s

$(1 - w_o) \approx 0.1$

ρ = 1.9905 lbf-sec^2/ft^4, 1025.9 Kg/m^3

Blade chord lengths for the new impeller were set at approximatley 75% of those of the standard impeller to maintain the same expanded blade area ratio, A_E/A_o. Final propeller geometry was obtained by applying lifting surface corrections[8] to the lifting line program design results. Table 3 lists the final new impeller geometry. Since all calculations assumed a cylindrical hub shape and a non-raked impeller, the new impeller was constructed with a 15.2 degree forward rake in order that the blades would be normal to the hub profile at the blade/hub intersection. In the final steps of impeller construction, the

---

[8] Morgan, W. B. et al., "Propeller Lifting-Surface Corrections," Trans. SNAME, Vol. 76 (1968)

impeller tips were cut to obtain a proper fit with the waterjet wear ring for a prescribed impeller axial position relative to that wear ring.

EXPERIMENTAL PROCEDURE

CALIBRATION

Calibration of the torque meter, rpm counter, trim gage, and load cell for bollard tests was conducted by NAVSECNORDIV. The torque meter was an S. Himelstein Model MCRT6-02T-15-3 with a range of 0 - 1500 in-lbs (0 - 169.5 N.m) and an accuracy of $\pm$ 0.4 percent full scale. The load cell used during bollard experiments was a Dillon Model 100 with a range of 0 - 4000 lbs (17793.N) and an accuracy of $\pm$ 0.5 percent full scale. The rpm counter was a magnetic pickup sensing the gear teeth of a rotating gear attached to the pump shaft. The accuracy of the device was limited only by the operator recording the rpm and is estimated to be $\pm$ 5 rpm. Trim was measured by visually inspecting a bubble in a hemispherical tube calibrated in degrees. The accuracy is estimated to be $\pm$ 0.2 degrees.

Pressure probes located in the inlet of the waterjet and at the exit nozzle were installed and calibrated by DTNSRDC personnel. A complete description of these probes and their calibration can be found in Reference 2. The pressure probes were calibrated statically and dynamically. Dynamic calibrations at the conclusion of testing were performed in DTNSRDC - Langley Tank No. 1 over a speed range of

15 - 30 ft/sec (4.57 - 9.14 m/sec). Results of this calibration indicated a relationship between probe measured velocity and angle of inflow velocity as indicated in Figure 4.

TEST PROCEDURES

Experiments as summarized in Tables 4, 5, and 6 were conducted under six separate conditions. There were two impellers and two nozzles available for the tests. The standard impeller was used with the standard 5.75 in. diameter (0.146 m) nozzle while the DTNSRDC impeller was used with the 5.75 in. nozzle and 6.00 in. (0.152 m) nozzle. The three resulting groups were further broken down into a bollard test and an underway test. Bollard tests were conducted with the boat tied to the dock. Underway tests were conducted in open water on a previously layed out course of 4107 feet (1251.8 m) running on a line 30 deg Southeast. The water depth varied from 7 to 9 feet (2.1 - 2.7 m) and the craft displacement was maintained at 15,600 lbs (69,392 N). During the underway tests the boat traversed the course twice, once in each direction at the same pump rpm settings. At the end of each set of underway runs, special conditions were set by running the starboard engine at a different rpm level than that of the port engine. All tests were conducted under the same approximate sea conditions.

DATA ACQUISITION

Due to a limited space aboard the test craft, the pressure data were recorded on a Honeywell 5600C Analog Tape Recorder and played back to a shore-based computer after testing. Prior to being recorded the data signals were conditioned using Model 4470 Endevco signal conditioners and Dana amplifiers. Data were analyzed using an Interdata Model 70 mini-computer with 32K memory. Interfaced with the computer was an Analogic 5800 14-bit analog to digital converter. Included in the system was a high speed printer, ASR-33 teletype, and a Kennedy Model 3110 9-track digital tape deck. Torque, rpm, trim, and load cell readings were visually recorded by NAVSECNORDIV personnel. Torque, rpm, and load cell outputs were displayed using a digital voltmeter.

During testing, initial data zeroes were collected for all channels with the starboard engine off and the port engine idling. Data were collected continuously throughout a run making it necessary to provide a marker on tape indicating when the traversing probes were in position. This was accomplished by the use of a switching box which could be triggered to either a positive or negative voltage. The switch was triggered positive for approximately ten seconds after setting the position of the probes.

The analog data were played back to the computer system, digitized at a rate of 100 samples per second, and stored on magnetic tape

using a continuous data collection package developed at DTNSRDC. Data averaging and further analysis was accomplished using both the Interdata mini-computer and a CDC 6600 high speed computer.

RESULTS AND DISCUSSION

The flow measurements were computed from local static and total pressure measurements taken in the inlet as indicated in Figure 2. As a backup to these upstream measurements flow rate was also computed from a total head pressure probe which traversed the exit nozzle. In the analysis it was assumed that Bernoulli's equation applies or that $V_i = \sqrt{(p_t - p_s)2/\rho}$. For the nozzle velocity computation the static pressure was assumed to be atmospheric pressure. The nozzle velocities were integrated over the nozzle radius assuming a concentric flow field. The inlet velocities could not be integrated in this manner because of the non-uniformity of the velocity from the bottom of the duct to the top. The inlet velocities were integrated by dividing the inlet area into smaller local areas surrounding the local pressure measurements. The grid system in Figure 2 displays these local areas. The results of upstream integrated measurements along with the nozzle integrated flow rate for the standard impeller are presented in Figure 5. As displayed, the upstream flow rate (integrated) was greater than the nozzle flow rate for underway tests. It should also be noted that the upstream

integrated flow rate for the bollard condition was greater than the flow rate computed from the bollard thrust measurement using the equation $T_b = \rho Q^2/A_j$. The discrepancies between mass flow rates determined from integration of velocities over an area upstream of the impeller and those flow rates determined from integration of flow over the nozzle area (or flow rates calculated from bollard thrust measurements) could arise from one or both of the following:

-- flow angularity into the measuring transducers due to the inlet angle

-- inaccuracies in the integration due to the limited number of stations at which local velocity could be measured.

The discrepancies, however, appeared to be a constant percentage of mass flow regardless of rpm. By adjusting the underway upstream integrations with the constant multiplier of 0.852, the results matched the underway nozzle integrated flow rate. The same multiplier was applied to the bollard upstream integrated flow rate and the results then matched the computed flow rate from measured bollard thrust using the equation $T_b = \rho Q^2/A_j$. The adjustment of upstream flow rate data is shown in Figure 6 along with nozzle integrated data and flow rate calculated from bollard thrust data.

Figures 7 and 8, which are the flow rates computed for the DTNSRDC impeller experiments, have presented upstream flow rates with adjustments using the same multiplier of 0.852.

The results of the powering tests are presented in Figures 9, 10, and 11. Figure 9 presents the shaft rpm vs shaft power for

underway conditions of each pump configuration. The results indicate that the standard impeller turned at a higher rpm for a given shaft power than either of the other two configurations involving the DTNSRDC impeller. In Figure 10 where shaft power data are represented versus craft speed, it is evident that less power is required to drive the craft at a given velocity with the standard impeller. The DTNSRDC impeller with the 6.0 in. (0.152 m) nozzle did perform better than with the 5.75 in. (0.146 m) nozzle. The experimental conditions for each of the underway configurations were the same in other respects as indicated by the trim vs velocity and rpm vs velocity curves presented in Figure 10. Experimental results for each of the pump configurations at bollard conditions are presented in Figure 11. The standard impeller performed better than the DTNSRDC impeller in producing thrust at bollard conditions. A higher rpm and a higher thrust were achieved by the standard impeller for the same shaft power. The large 6.0 in (0.152 m) nozzle improved the performance of the DTNSRDC impeller.

Having examined the propulsion data through conventional graphical representations a different approach was adapted in order to discover why the DTNSRDC impeller was less efficient than the standard impeller. This lead to investigating methods which applied the energy-in versus energy-out principle. One approach was to take the pump flow rate as representative of the output energy and the

shaft power as representative of energy input. The results of this analysis are presented in Figure 12 for the bollard experiments and Figure 13 for the underway experiments. The bollard experiments indicated that the DTNSRDC impeller performed as well or better than the standard impeller in producing mass flow, however, the superior performance was not reflected in the underway runs of Figure 13. This would suggest that the DTNSRDC impeller was more adversely affected by the inflow velocity distribution of the inlet. Another reason for the lower performance of the DTNSRDC impeller might be that neither the stators nor the nozzle were redesigned to match the new impeller design.

In further analysis of the waterjet performance, the net thrust was computed from flow rate using the equation $T_n = \rho Q^2/A_j - \rho Q V_s$. Figures 14, 15, and 16 present this data along with the measured thrust data from the bollard experiments. There are two interesting results from this data. First it was noted that the underway thrust was greater than bollard thrust (at the same rpm) below planing speed. This same trend was found in data collected by D.W. Hankley[9]. The second noticeable result was the sudden drop in net thrust as the boat achieved a planing condition. This drop in calculated net thrust occurs due to the craft speed dependency in the equation $T_n = \rho Q^2/A_j - \rho Q V_s$. The onset of the net thrust drop corresponds to

---

[9] Hankley, W. W., "Full Scale Propulsion Characteristics of Two Marine Waterjets Rated at 500 hp and 1050 hp," NAVSECNORDIV Report No. 6660-6 (Jan 1971)

the speed at which the craft achieves a planing condition. The drop is accentuated in the speed range in which craft resistance varies little with speed and in which significant speed increase is obtainable with small increases in input power and pump rpm.

CONCLUSIONS AND RECOMMENDATIONS

1. Mass flow measurements were made and three waterjet unit configurations were evaluated in full scale craft underway and bollard experiments. Overall waterjet performance has been reported in this report and details of the waterjet inlet inflow velocity distributions have been reported under separate cover[2]. The results shown in both reports indicate that:

   -- inlet velocity distributions and consequent mass flows through flush inlet waterjets are significantly different in underway and stationary (bollard) conditions. This suggests that predictions of underway waterjet performance from stationary "test-stand" data or from pump performance characteristics are susceptible to error.

   -- detailed velocity measurements within the waterjet inlet and across the exit nozzle, during underway operation, appear to be the best method for the evaluation of waterjet inlet performance and overall waterjet performance.

2. It does not appear practical to utilize current marine propeller design techniques for the design of waterjet impellers. This is primarily due to the very high power absorption of waterjet units

for relatively small impeller/stator disk areas and the fact that present propeller design procedures are based on moderately loaded propeller design theory. This statement does not necessarily apply to future waterjets which might have high inlet velocity-to-craft velocity ratios and low ducting losses nor does it apply to potential hybrid propulsor configurations such as partially shrouded propellers operating in deep tunnels.

3. With regard to the experimental results reported in this report and Reference 2:

-- the DTNSRDC impeller performed better overall with the 6.0 in. (0.152 m) nozzle than with the 5.75 in. (0.146 m) nozzle but it did not exceed the performance of the standard impeller and 5.75 in. (0.146 m) nozzle. Possible explanations for this would be the lack of redesign of stators and nozzle to match the new impeller.

-- the DTNSRDC impeller with 6.0 in. (0.152 m) nozzle was equal or better in producing mass flow at given horsepower than the standard impeller during bollard experiments; however, this was not reflected in the underway experiments. The non-uniform velocity flow into the inlet appeared to more heavily influence the performance of the DTNSRDC impeller.

-- a redesign of the inlet would appear to have the greatest potential for increasing the overall performance of the waterjet system used in these experiments.

REFERENCES

1. Brandau, J. H., "Performance of Waterjet Propulsion Systems - A Review of the State-of-the-Art," Journal of Hydronautics, Vol. 2, No. 2, pp. 61-76 (April 1968).

2. Alder, R. S., "Inlet Velocity Distribution of a Full Scale Flush Inlet Waterjet," DTNSRDC Ship Performance Department Report SPD-718-01 (Aug 1976).

3. Larbs, H. W., "Moderately Loading Propellers with a Finite Number of Blades and an Arbitrary Distribution of Circulation," Trans. SNAME, Vol. 60, pp. 73-117 (1952).

4. Cheng, H. M., "Hydrodynamic Aspect of Propeller Design Based on Lifting-Surface Theory, Part I, Uniform Chordwise Load Distribution," David Taylor Model Basin Report 1802 (Sep 1964).

5. Cheng, H. M., "Hydrodynamic Aspect of Propeller Design Based on Lifting-Surface Theory, Part II, Arbitrary Chordwise Load Distribution," David Taylor Model Basin Report 1803 (Jun 1965).

6. Kerwin, J. E. and R. Leopold, "Propeller-Incidence Correction Due to Blade Thickness," J. Ship Research, Vol. 7, No. 2 (Oct 1963).

7. Caster, E. B., "A Computer Program for Use in Designing Ducted Propellers," Naval Ship Research and Development Center Report 2507 (Oct 1967).

8. Morgan, W. B. et al., "Propeller Lifting-Surface Corrections," Trans. SNAME, Vol. 76 (1968).

9. Hankley, D. W., "Full Scale Propulsion Characteristics of Two Marine Waterjets Rated at 500 hp and 1050 hp," NAVSECNORDIV Report No. 6660-6 (Jan 1971).

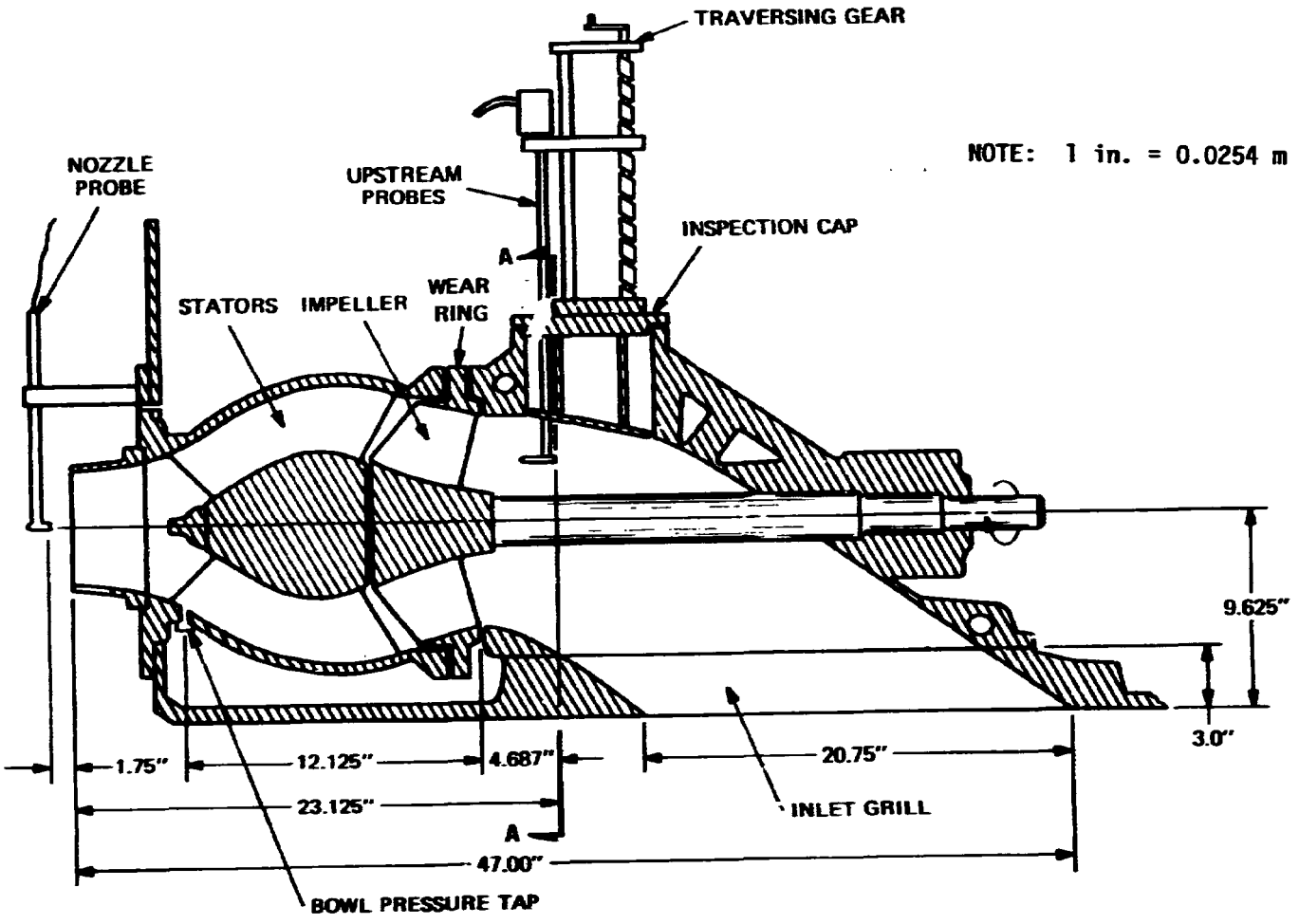

Figure 1 - Waterjet Pump Profile

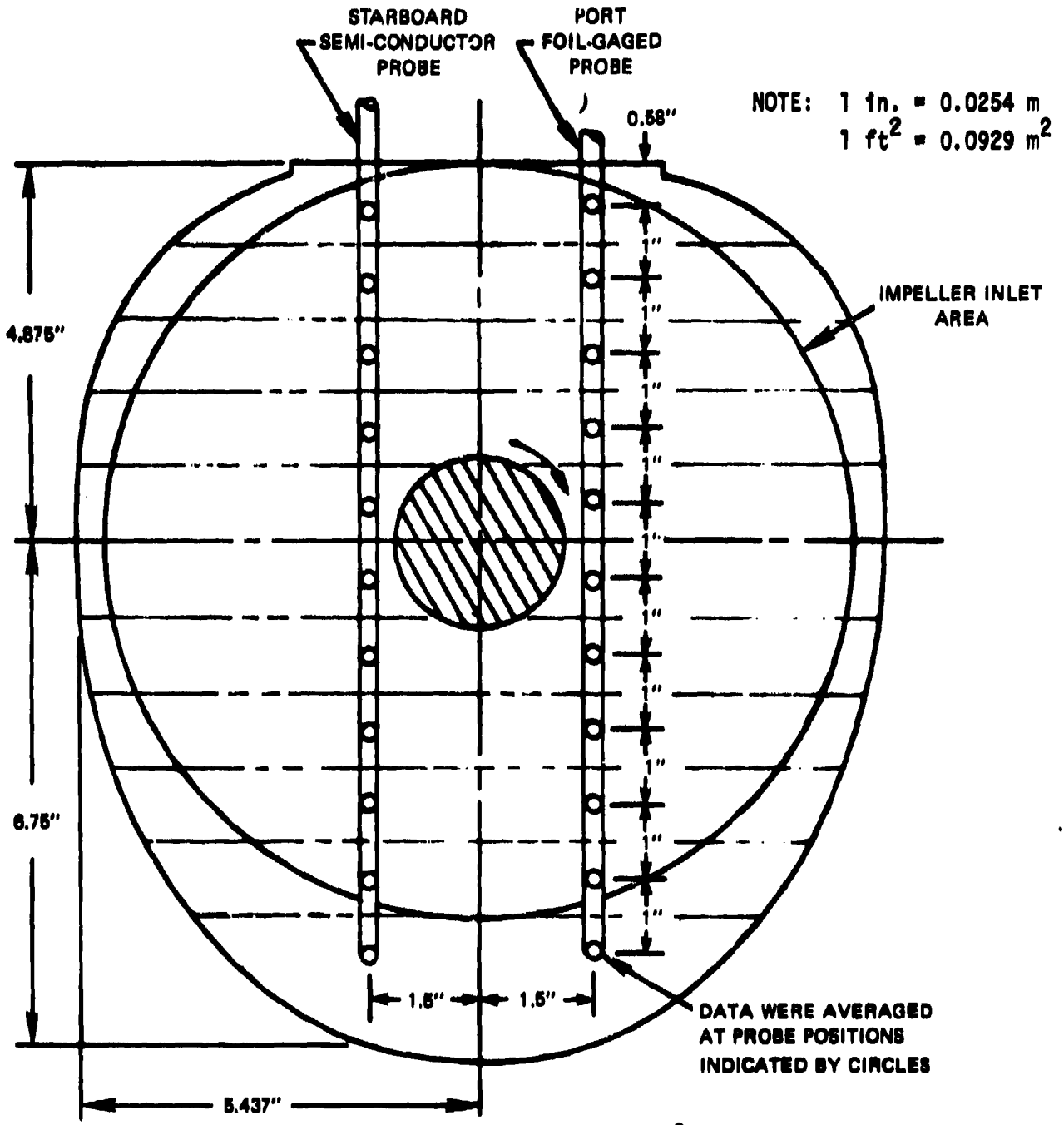

Figure 2 - Cross Section of Duct in the Plane of the Traversing Probes

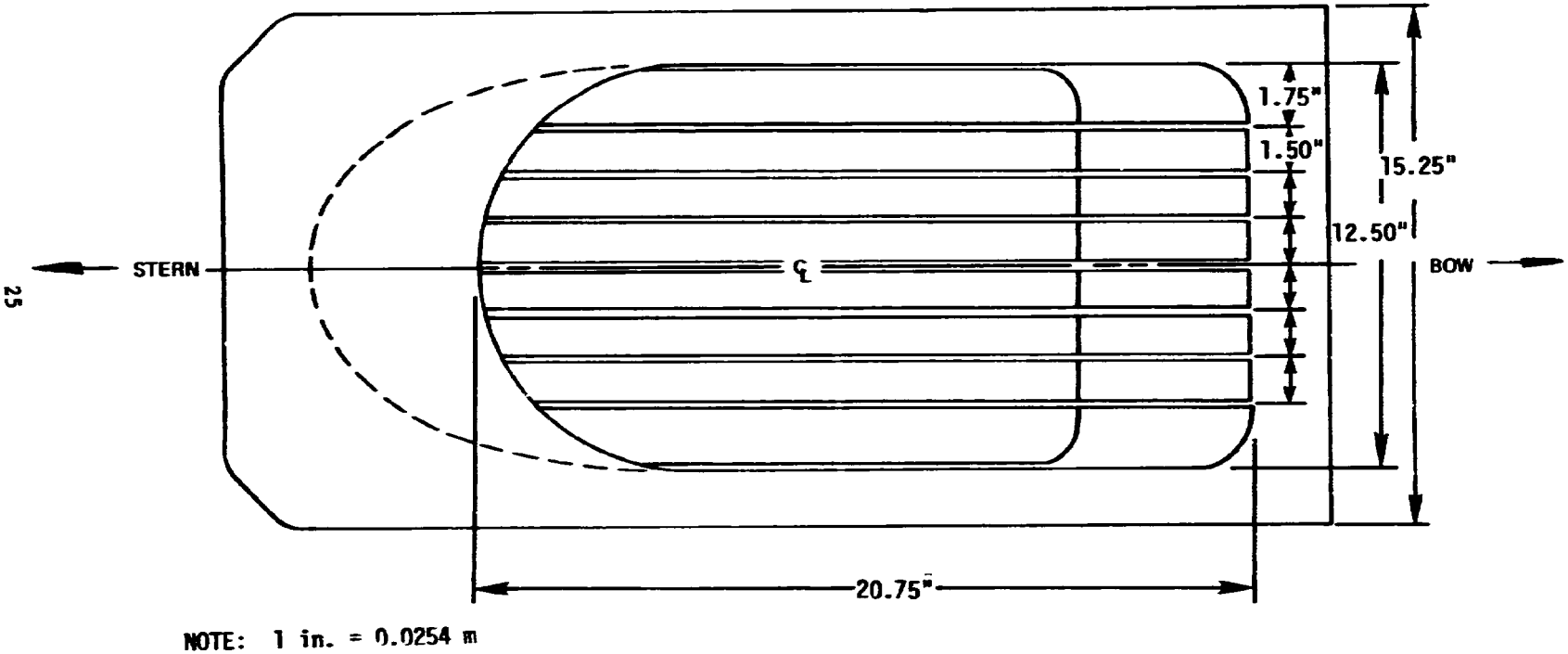

NOTE: 1 in. = 0.0254 m

Figure 3 - Waterjet Inlet and Grating

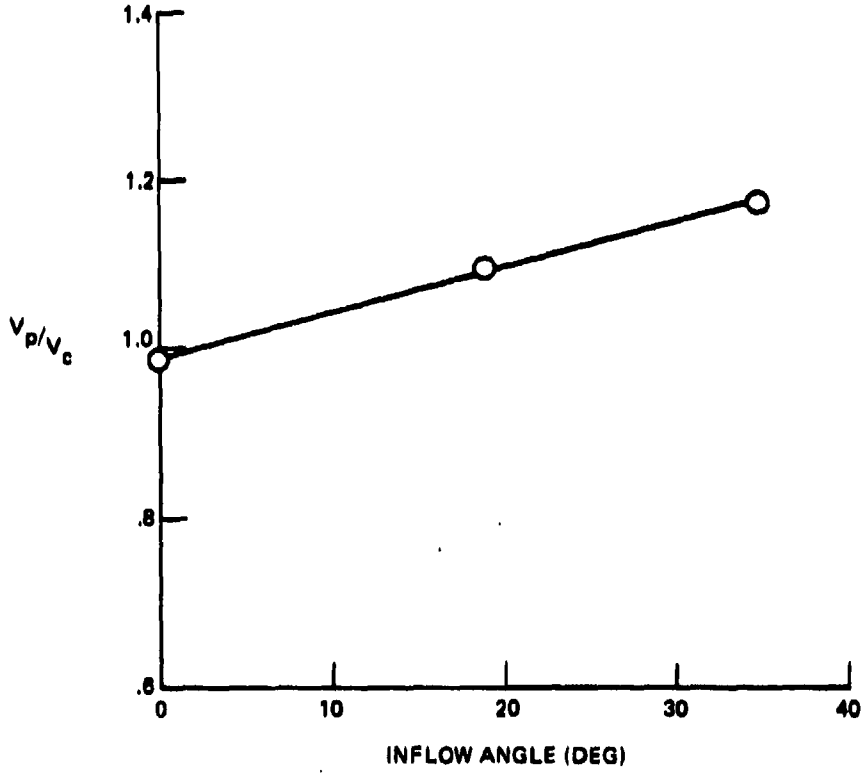

Figure 4 - Ratio of Probe Measured Velocity to Carriage Velocity for Various Degrees of Inflow Angle

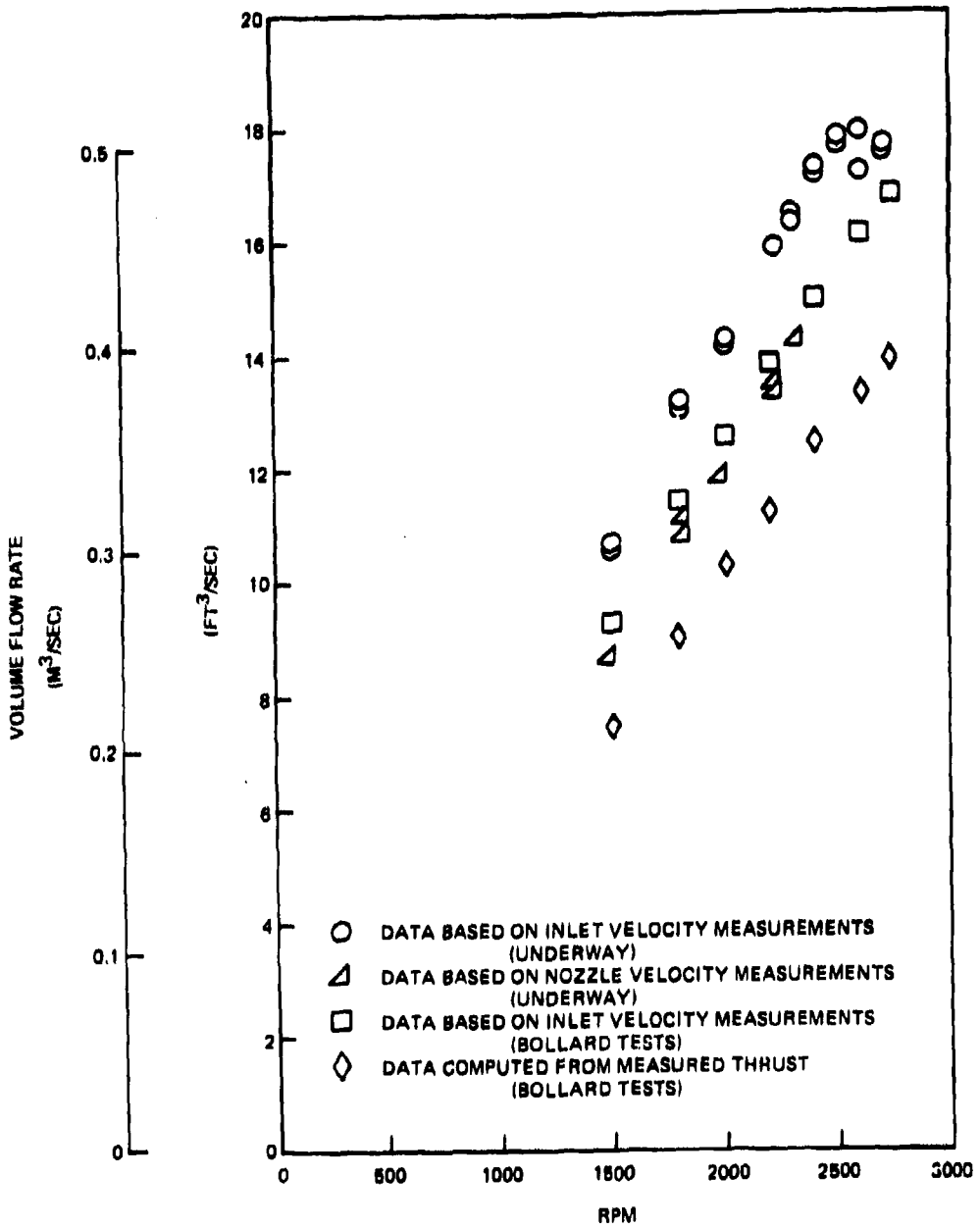

Figure 5 - Volume Flow Rate Data for Standard Impeller with 5.75 in. (0.146 m) Nozzle

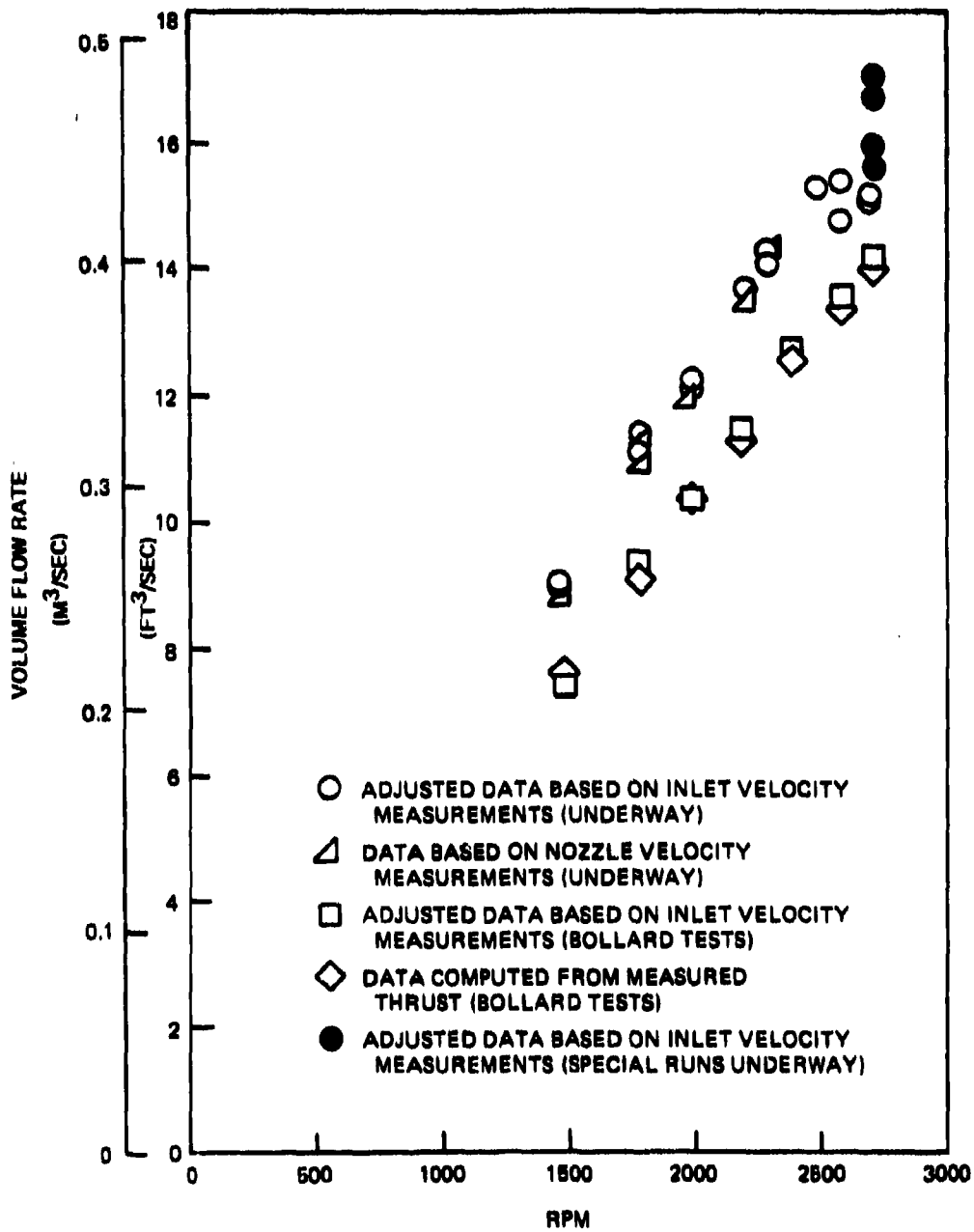

Figure 6 - Adjusted Volume Flow Rate Data for Standard Impeller with 5.75 in. (0.146 m) Nozzle

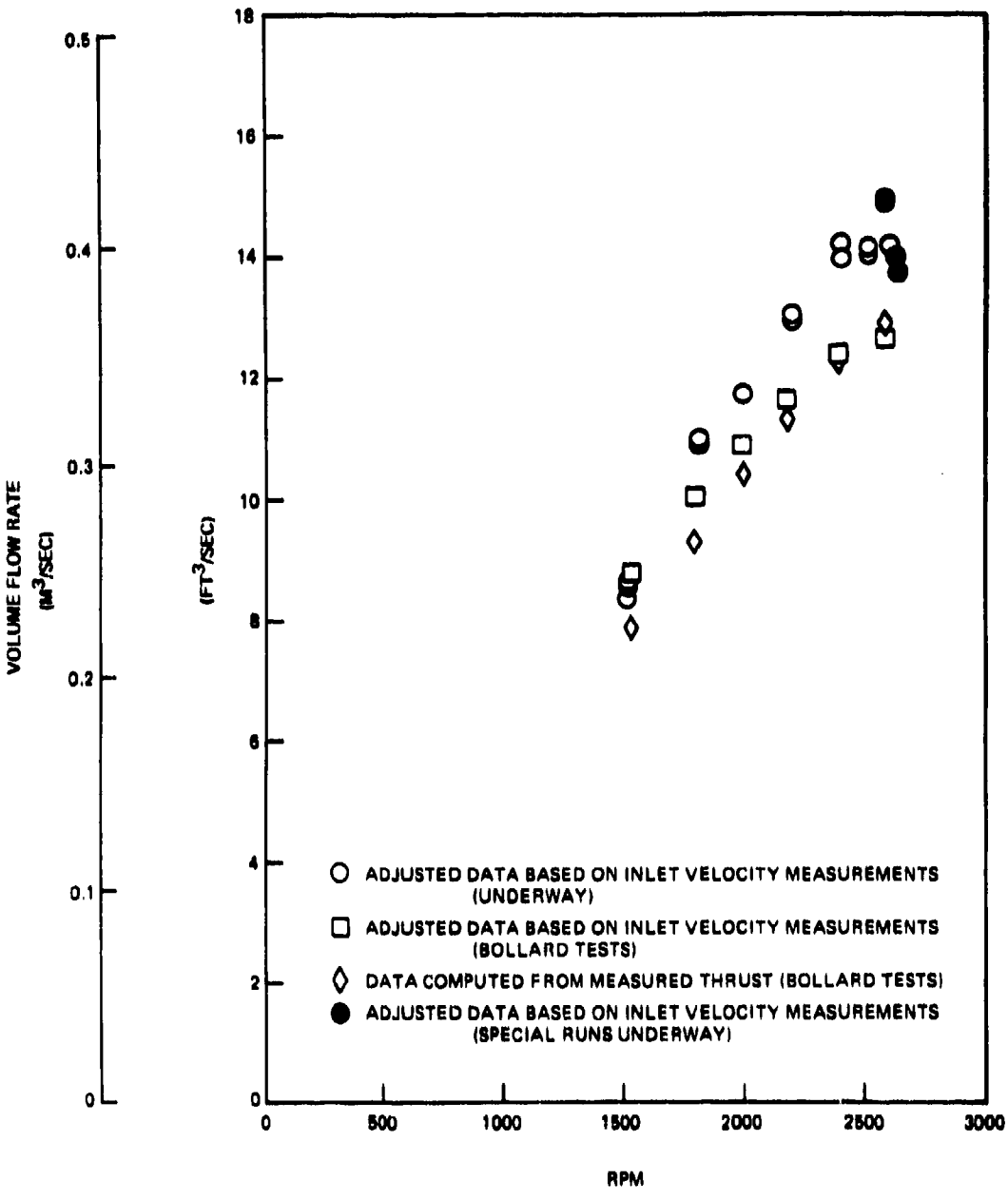

Figure 7 - Volume Flow Data for DTNSRDC Impeller with 5.75 in. (0.146 m) Nozzle

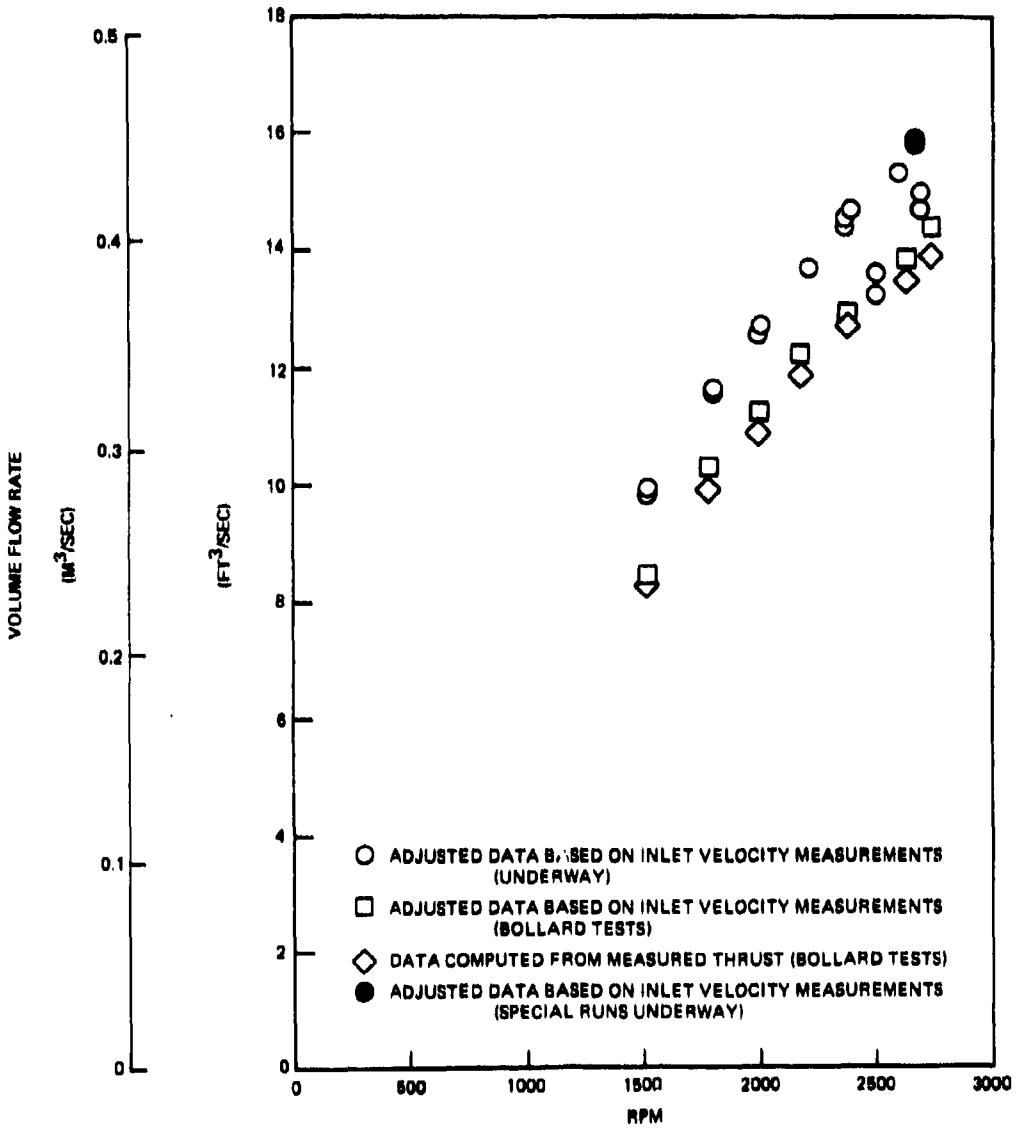

Figure 8 - Volume Flow Rate Data for DTNSRDC Impeller with 6.0 in. (0.1524 m) Nozzle

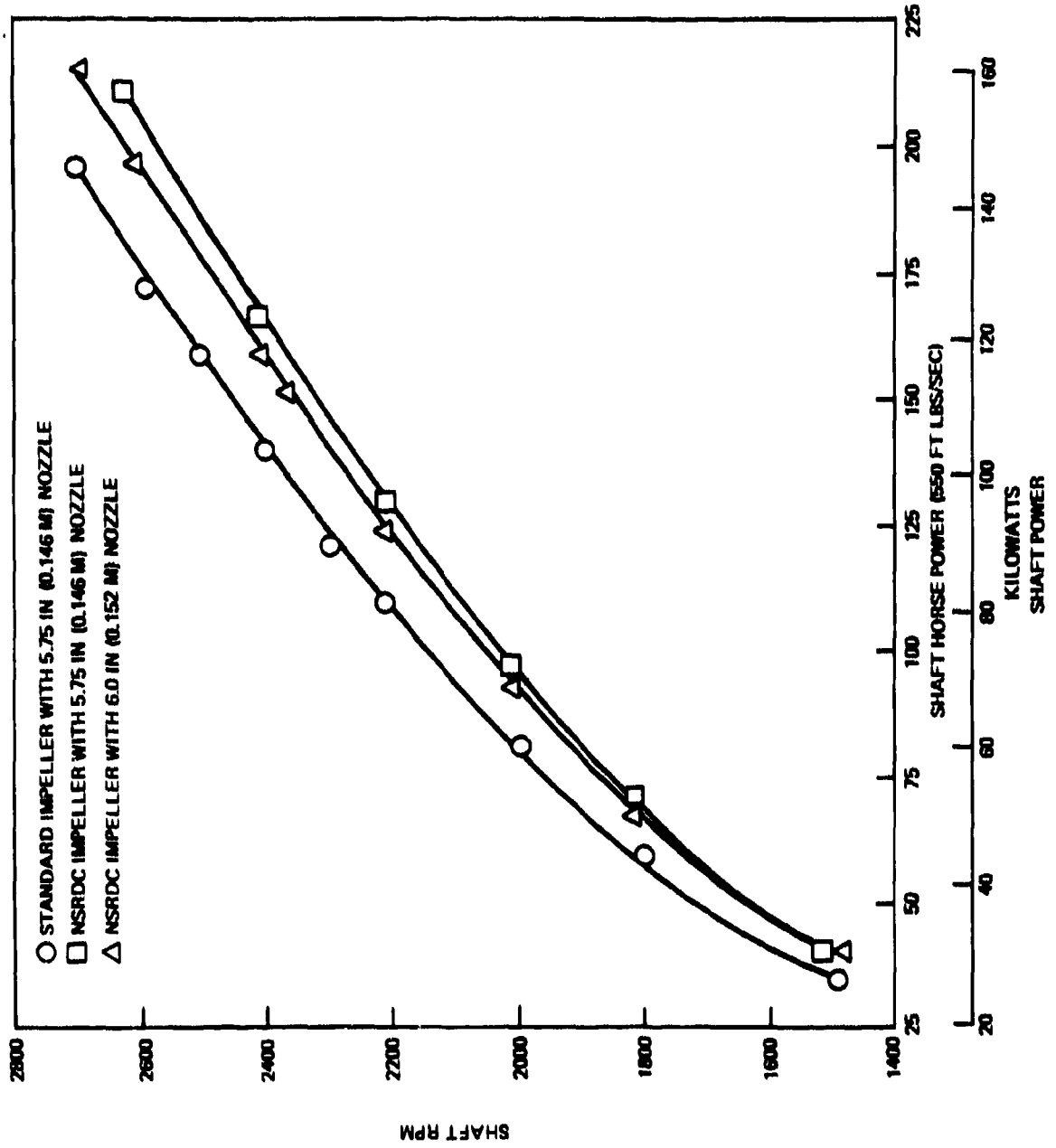

Figure 9 - RPM Versus Shaft Power for Underway Experiments

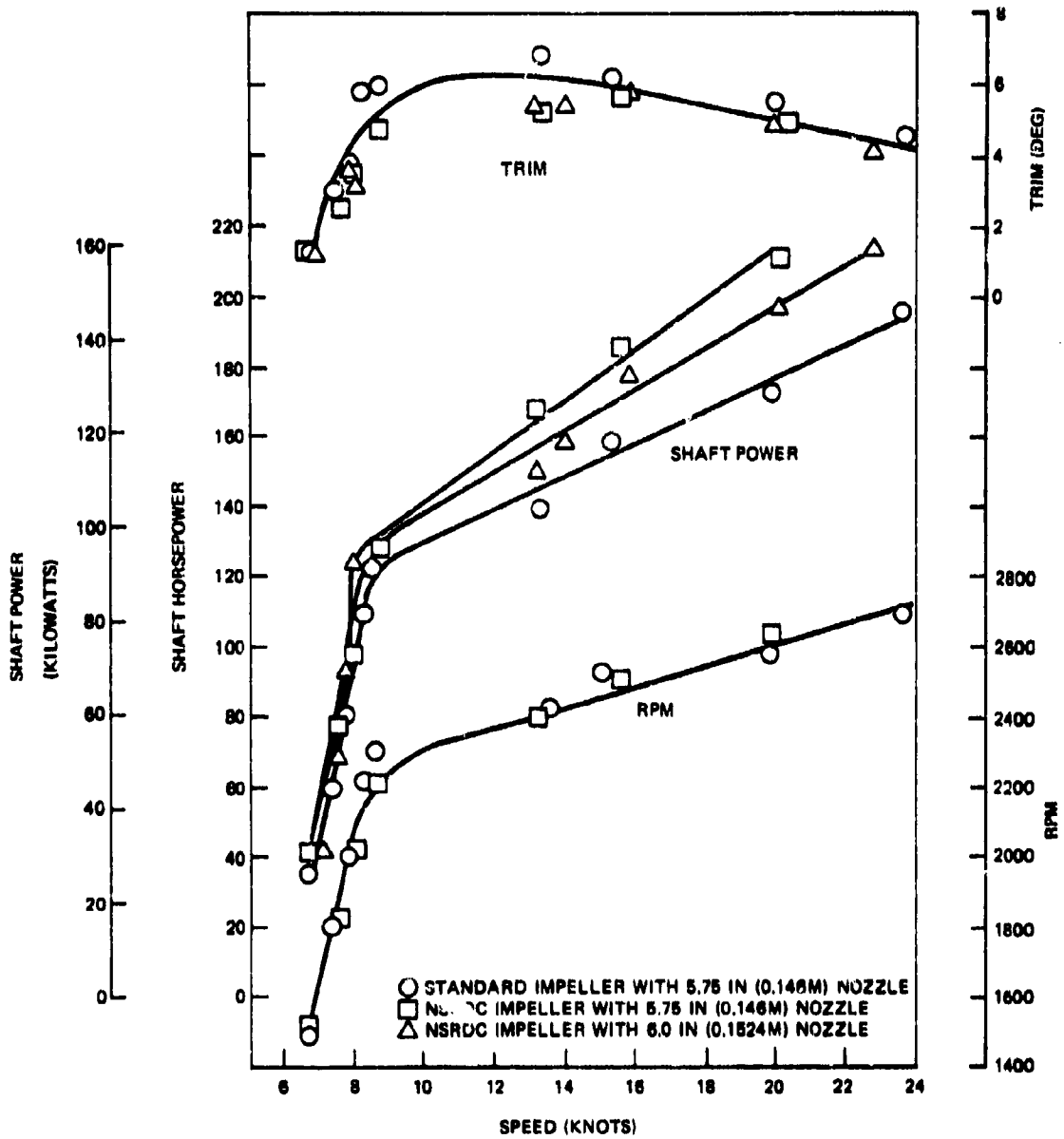

Figure 10 - RPM, Trim, and Shaft Power Versus Craft Speed

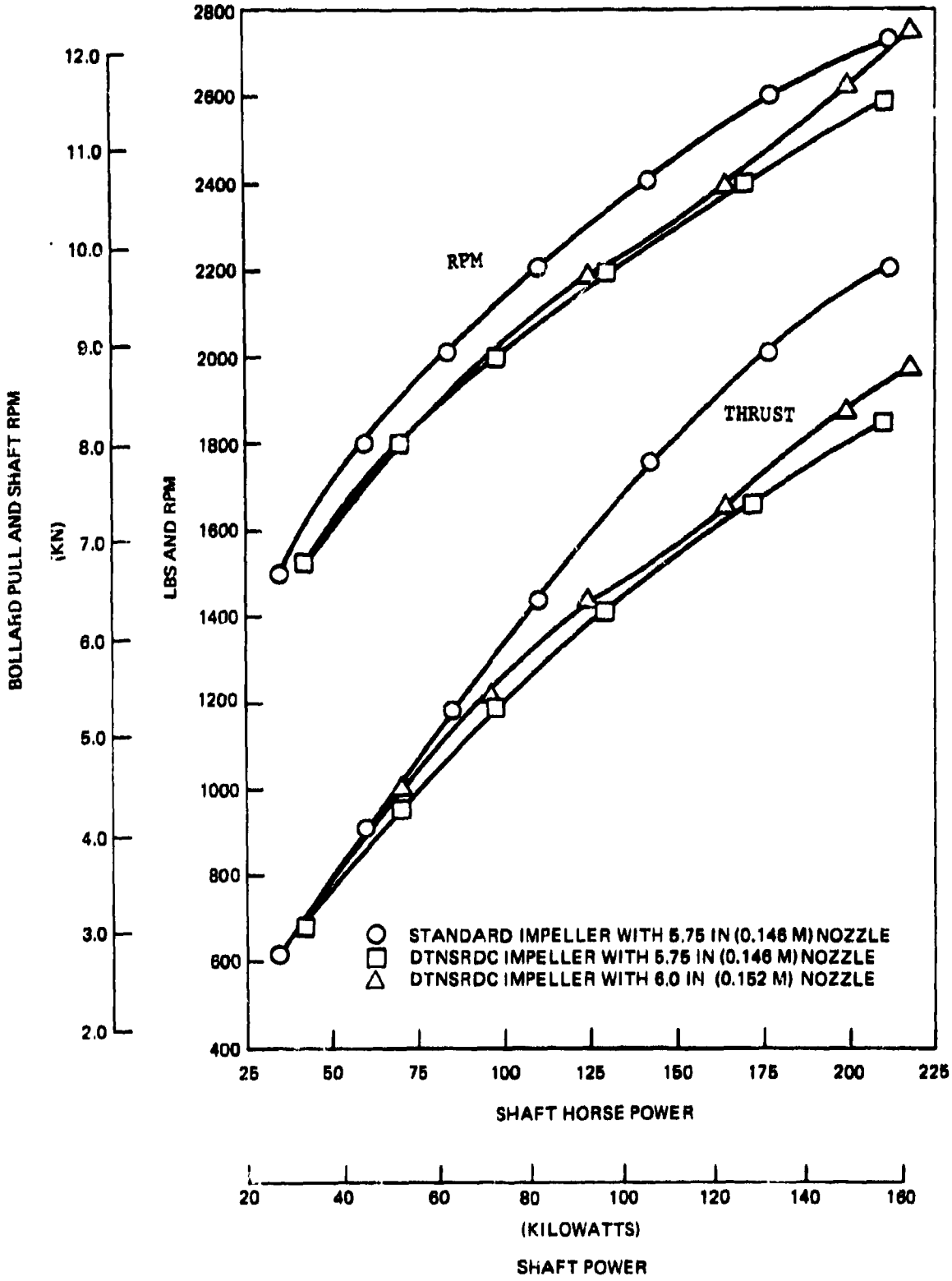

Figure 11 - Thrust and RPM Versus Shaft Power for Bollard Experiments

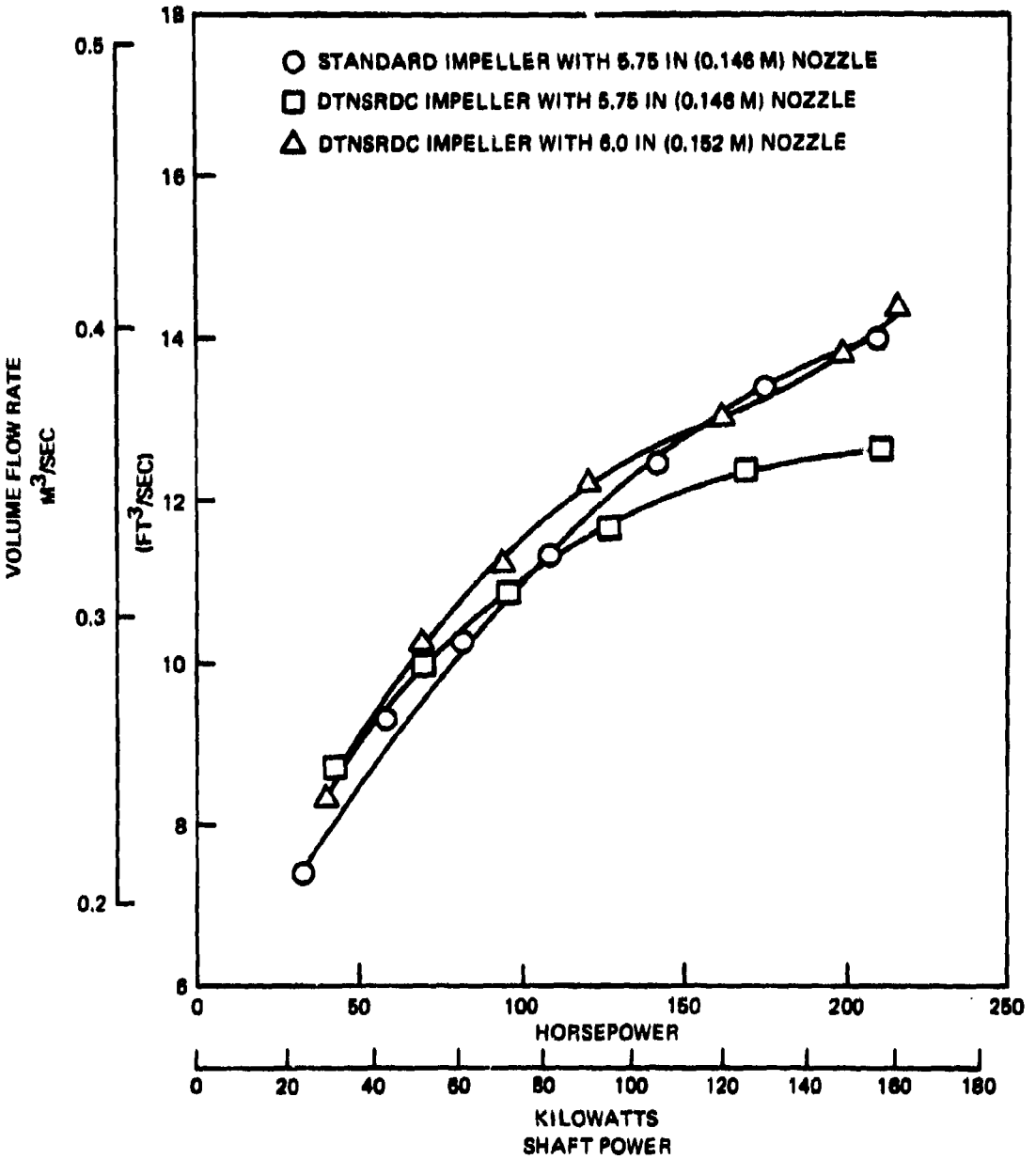

Figure 12 - Volume Flow Rate Versus Shaft Power for Bollard Experiments

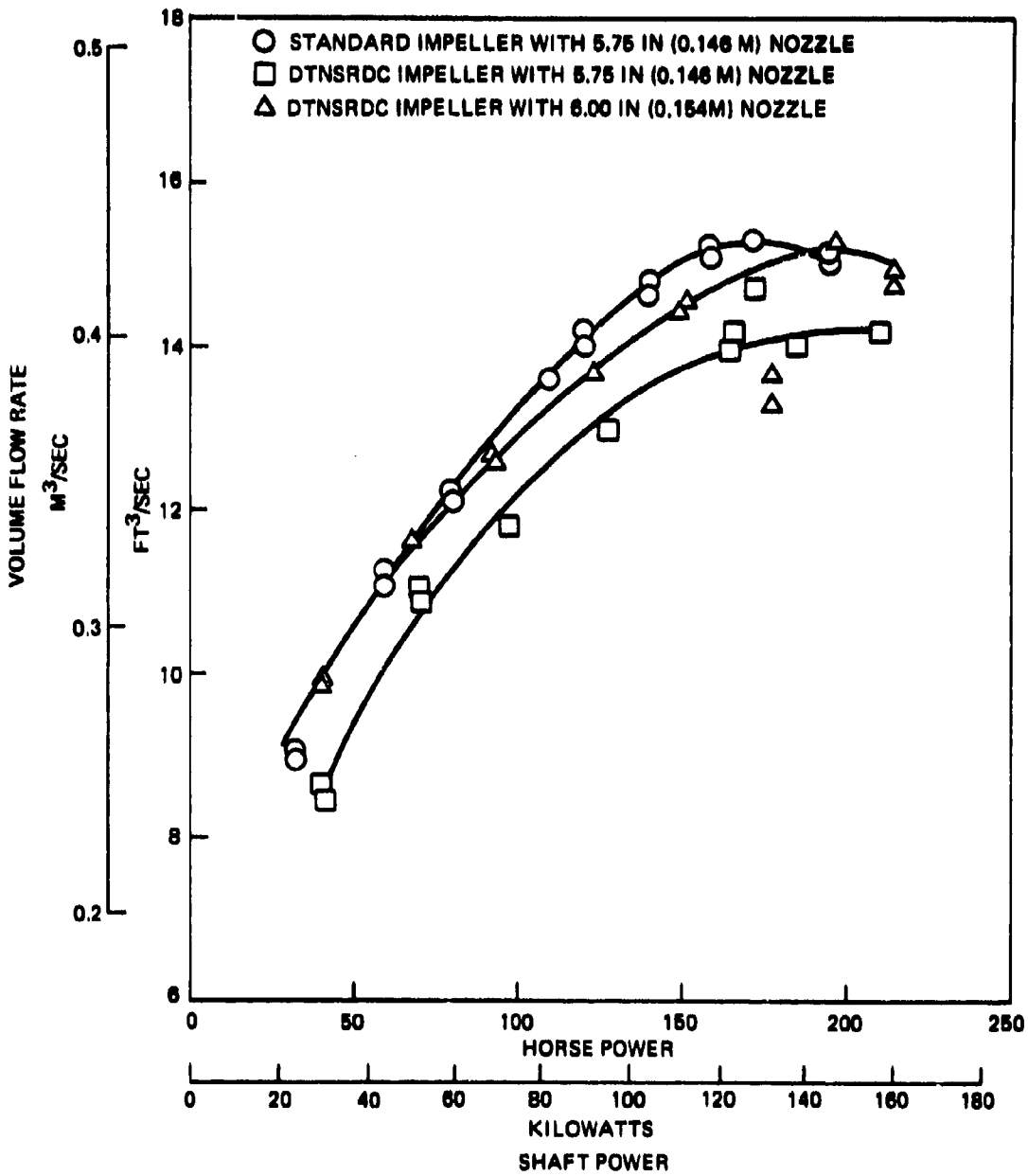

Figure 13 - Volume Flow Rate Versus Shaft Power for Underway Experiments

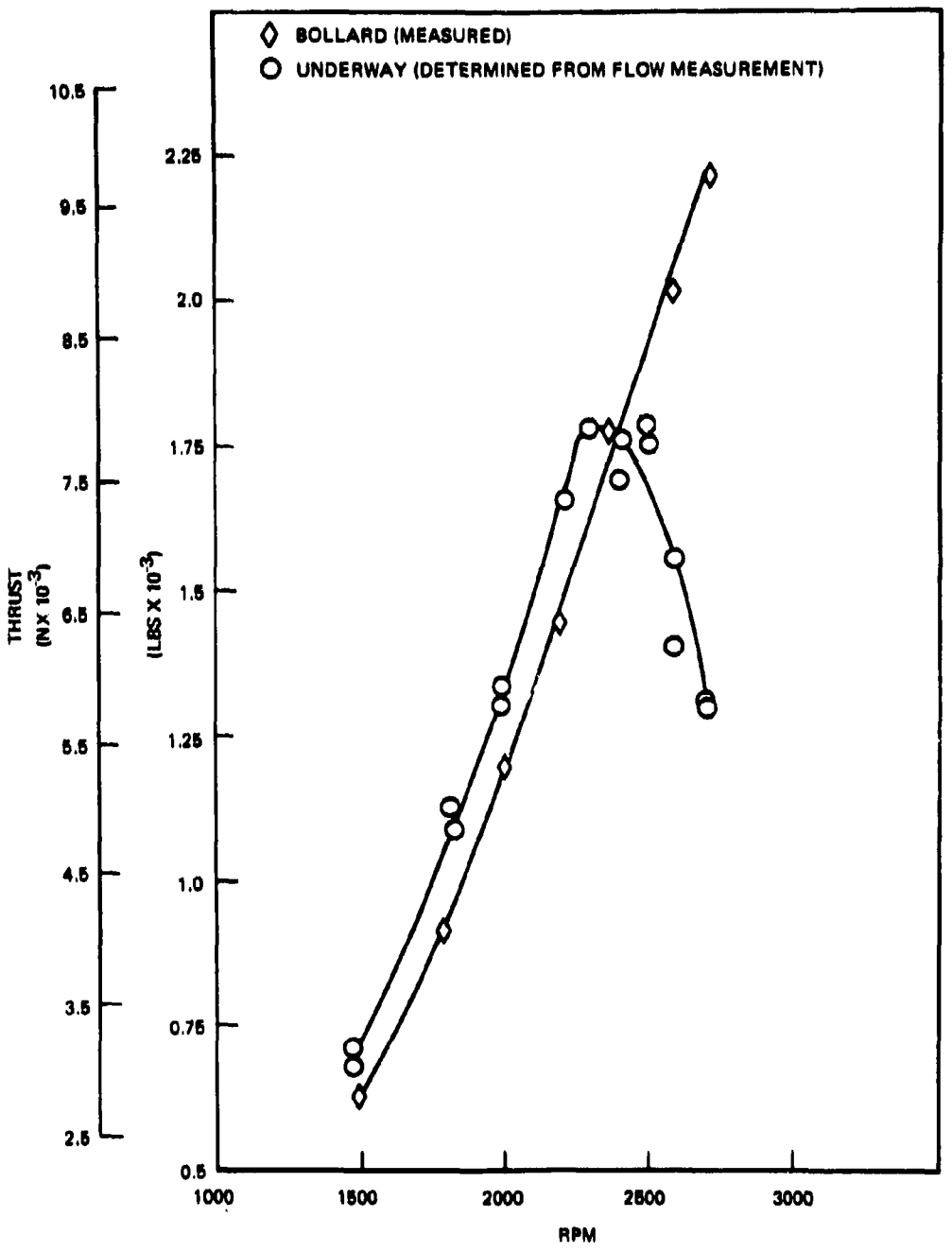

Figure 14 - Thrust Versus RPM for Standard Impeller with 5.75 in. (0.146 m) Nozzle

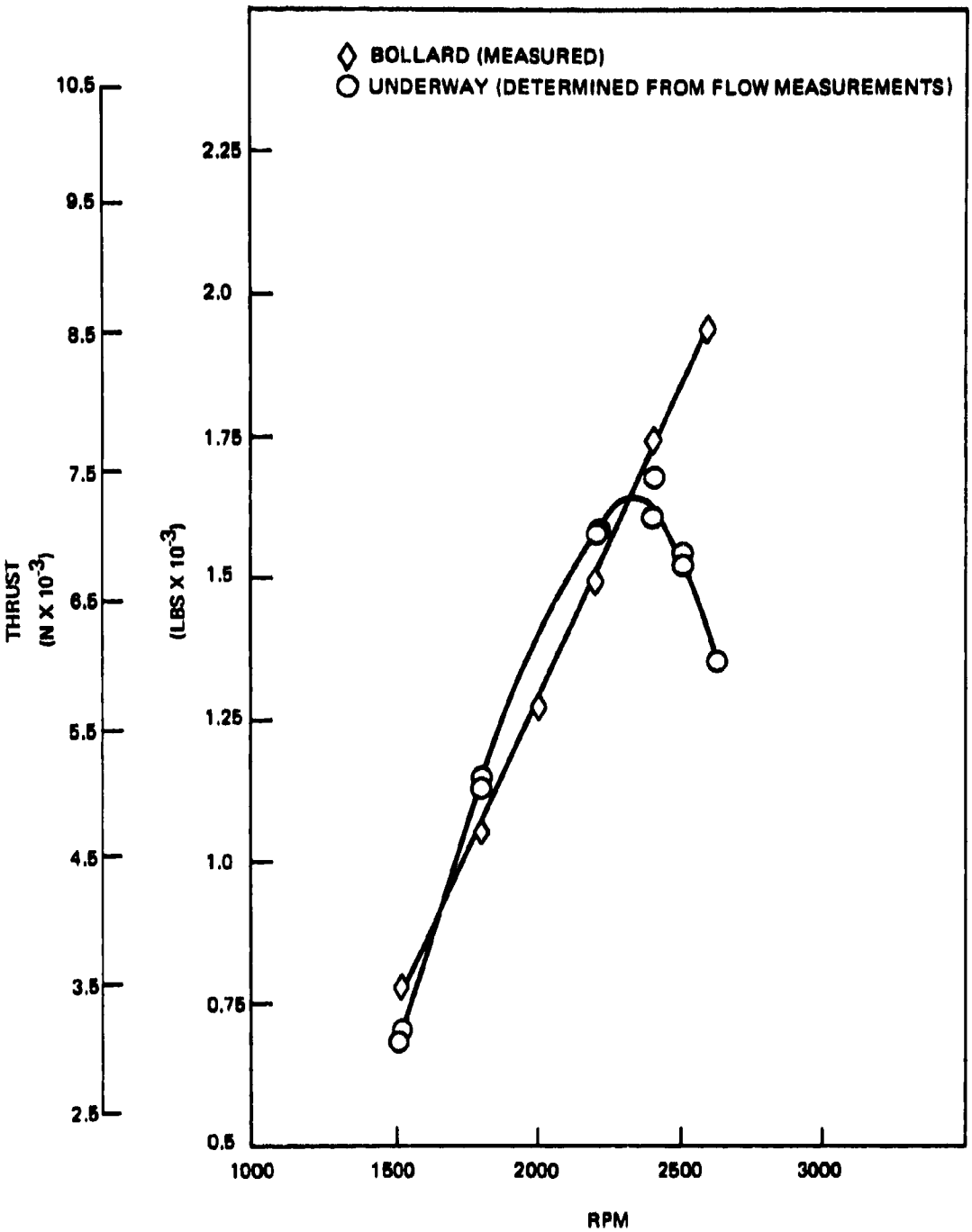

Figure 15 - Thrust Versus RPM for DTNSRDC Impeller with 5.75 in. (0.146 m) Nozzle

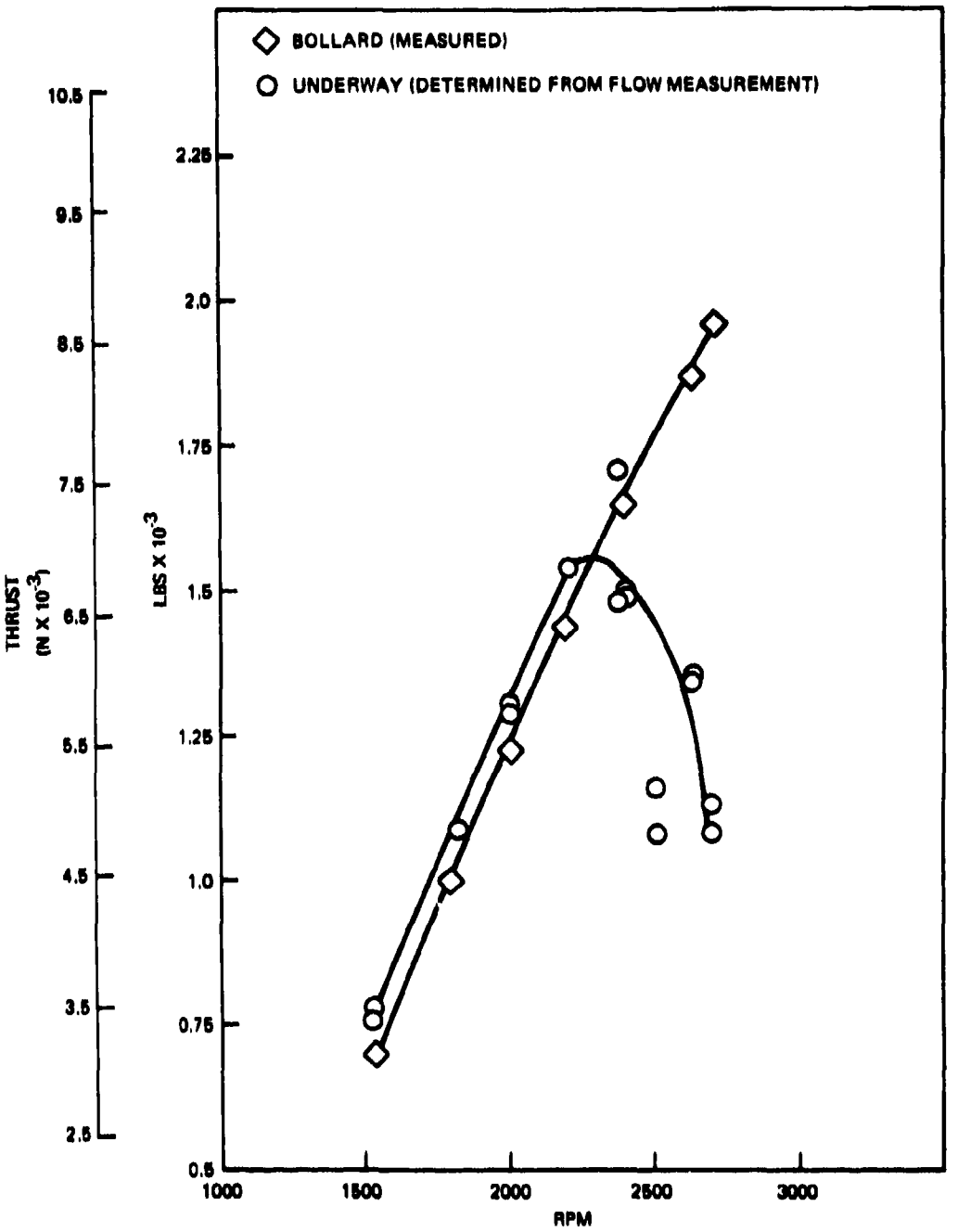

Figure 16 - Thrust Versus RPM for DTNSRDC Impeller with 6.0 in. (0.1524 m) Nozzle

TABLE 1 - TEST CRAFT

Length	31 ft (9.45 m)
Beam	10 ft 7 in. (3.23 m)
Weight	15,600 lb (69,392 N)
Construction	V-Bottom Planing Hull
Propulsion	2 Diesel Engines 216 hp (161 kW) at 2800 rpm

TABLE 2 - STANDARD IMPELLER

Number of Blades	3
Maximum Diameter	11.85 in. (0.301 m)
Expanded Blade Area Ratio A_E/A_o	.7758

x	P/D	f_M/c	c/D	t/D
.5	1.0067	.0317	.7879	.0283
.6	.9632	.0299	.8718	.0275
.7	.9141	.0270	.9456	.0285
.8	.8584	.0239	1.0125	.0292
.9	.8728	.0173	.7024	.0311
1.0	----	----	0	.0051*

*NOTE: The extreme outer diameter of the impeller contacts the wear ring at a single point.

TABLE 3 - DTNSRDC NEW DESIGN IMPELLER

Number of Blades	4
Maximum Diameter	11.85 in. (0.301 m)
Expanded Blade Area Ratio A_E/A_o	.7758
Rake Angle	-15.2 deg

x	P/D	f_M/c	c/D	t/D
.5	.8425	.0322	.5904	.0250
.6	.8410	.0336	.6600	.0250
.7	.8430	.0343	.7130	.0250
.8	.8540	.0347	.7595	.0256
.9	.9150	.0365*	.5268*	.0270
1.0	1.0500	.0500*	.4238*	.0051*

*NOTE: Approximation, the blades were cut to fit the wear ring.

TABLE 4 - EXPERIMENTS WITH STANDARD IMPELLER AND 5.75 IN. (0.146 m) NOZZLE

Run No.	Stbd. rpm	Shaft Horsepower	Velocity knots	Trim deg	Bowl Pressure psig	Thrust lbs	Comments
20	1490	34.4	6.7	1.25	9.0		
21	1490	34.4	6.7	1.25	9.0		
22	1806	59.7	7.4	2.75	13.5		
23	1803	59.7	7.4	2.75	13.5		
24	1997	80.4	7.8	3.75	16.5		
25	1996	80.4	7.8	3.75	16.5		
26	2218	109.7	8.3	5.75	20.5		
27	2213	109.7	8.3	5.75	20.5		
28	2301	121.4	8.6	6.00	22.0		
29	2296	121.4	8.6	6.00	22.0		
30	2409	139.9	13.3	6.75	24.8		
31	2408	139.9	13.3	6.75	24.8		
32	2514	158.9	15.3	6.25	27.5		
33	2516	158.9	15.3	6.25	27.5		
34	2596	172.4	19.9	5.50	30.0		
35	2591	172.4	19.9	5.50	30.0		
36	2700	196.0	23.6	4.50	33.0		
37	2699	196.0	23.6	4.50	33.0		
38	2710	198.0	11.9	6.50	32.0		Port rpm 1995
39	2700	195.0	13.4	5.75	32.0		Port rpm 1925
40	2702	196.0	19.5	5.00	32.0		Port rpm 2518
41	2701	194.0	21.9	5.00	32.0		Port rpm 2512
42	1499	34.8	0.0	0.00	10.0	626	
43	1799	59.9	0.0	0.00	14.0	909	
44	2009	83.0	0.0	0.00	17.5	1183	
45	2206	110.0	0.0	0.00	21.0	1440	
46	2409	142.7	0.0	0.00	25.0	1760	
47	2605	176.6	0.0	0.00	28.5	2012	
48	2736	211.0	0.0	0.00	32.0	2208	

NOTE: 1 psi = 6894 Pa 1 lbf = 4.448 N 1 hp = 745.7 W

TABLE 5 – EXPERIMENTS WITH DTNSRDC IMPELLER AND 5.75 IN. (0.146 m) NOZZLE

Run No.	Stbd. rpm	Shaft Horsepower	Velocity knots	Trim deg	Bowl Pressure psig	Thrust lbs	Comments
51	1520	42.3	0.0	0.00	11.5	685	
52	1799	69.9	0.0	0.00	15.3	958	
53	2008	97.5	0.0	0.00	19.5	1190	
54	2197	128.4	0.0	0.00	23.5	1410	
55	2405	168.5	0.0	0.00	28.0	1660	
56	2590	209.6	0.0	0.00	32.0	1850	
60	1511	41.9	6.7	1.25	12.25		
61	1507	41.9	6.7	1.25	12.25		
62	1809	70.7	7.6	2.50	17.3		
63	1806	70.7	7.6	2.50	17.3		
64	2014	97.8	8.0	3.50	22.0		
65	2013	97.8	8.0	3.50	22.0		
66	2206	128.8	8.7	4.75	24.0		
67	2203	128.8	8.7	4.75	24.0		
68	2416	166.6	13.3	5.25	29.0		
69	2410	166.6	13.3	5.25	29.0		
70	2505	185.2	15.6	5.75	31.0		
71	2504	185.2	15.6	5.75	31.0		
72	2623	211.6	20.1	5.00	34.0		
74	2634	212.7	22.2	4.50	34.5		Port rpm 2676
75	2629	210.7	22.3	4.50	34.5		Port rpm 2678
76	2582	207.0	9.3	5.75	34.0		Port rpm 2003
77	2578	205.0	9.3	6.00	34.0		Port rpm 2000

NOTE: 1 psi = 6894 Pa 1 lbf = 4.448 N 1 hp = 745.7 W

TABLE 6 - EXPERIMENTS WITH DTNSRDC IMPELLER AND 6.00 IN. (0.1524 m) NOZZLE

Run No.	Stbd. rpm	Shaft Horsepower	Velocity knots	Trim deg	Bowl Pressure psig	Thrust lbs	Comments
80	1509	41.9	0.0	0.00	10.0	700	
81	1798	69.8	0.0	0.00	13.5	1000	
82	2001	95.1	0.0	0.00	17.0	1225	
83	2186	123.5	0.0	0.00	20.0	1438	
84	2393	162.9	0.0	0.00	24.0	1650	
85	2623	197.6	0.0	0.00	27.0	1873	
86	2743	215.9	0.0	0.00	27.5	1970	
90	1518	40.9	6.9	1.20	10.0		
91	1516	40.9	6.9	1.20	10.0		
92	1808	68.2	7.5	2.50	14.0		
93	1808	68.2	7.5	2.50	14.0		
94	2009	93.4	7.8	3.50	17.0		
95	2010	93.4	7.8	3.50	17.0		
96	2211	123.6	8.0	5.25	20.8		
97	2207	123.6	8.0	5.25	20.8		
98	2363	152.0	8.5	7.00	23.6		Craft was not planing
99	2362	150.0	13.2	5.30	23.6		
100	2408	158.0	14.0	5.40	24.8		
101	2400	158.0	14.0	5.20	24.8		
102	2510	178.6	15.8	5.80	26.5		
103	2510	178.6	15.8	6.00	26.5		
104	2610	197.0	20.1	5.00	28.0		
105	2610	197.0	20.1	5.00	28.0		
106	2694	214.0	22.8	4.25	29.0		
107	2698	214.0	22.8	4.25	29.0		
108	2663	212.0	12.8	5.00	29.0		Port rpm 2010
109	2660	212.0	13.0	5.00	29.0		Port rpm 2010

NOTE: 1 psi = 6894 Pa 1 lbf = 4.448 N 1 hp = 745.7 W

DTNSRDC ISSUES THREE TYPES OF REPORTS

(1) DTNSRDC REPORTS, A FORMAL SERIES PUBLISHING INFORMATION OF PERMANENT TECHNICAL VALUE, DESIGNATED BY A SERIAL REPORT NUMBER.

(2) DEPARTMENTAL REPORTS, A SEMIFORMAL SERIES, RECORDING INFORMATION OF A PRELIMINARY OR TEMPORARY NATURE, OR OF LIMITED INTEREST OR SIGNIFICANCE, CARRYING A DEPARTMENTAL ALPHANUMERIC IDENTIFICATION.

(3) TECHNICAL MEMORANDA, AN INFORMAL SERIES, USUALLY INTERNAL WORKING PAPERS OR DIRECT REPORTS TO SPONSORS, NUMBERED AS TM SERIES REPORTS; NOT FOR GENERAL DISTRIBUTION.